3

NAL PROPOSAL No. 55

Correspondent: A. V. Tollestrup
Calif. Inst. of Tech.
Pasadena, Ca. 91109

FTS/Off-net: 213-688-2000
795-6841

# PROPOSAL TO STUDY $\pi^- p \to \pi^\circ n$ and $\pi^- p \to \eta n$ AT HIGH ENERGY

A. V. Tollestrup, R. L. Walker
Caltech

June 15, 1970

June 15, 1970

# PROPOSAL TO STUDY $\pi^- p \to \pi^o n$ and $\pi^- p \to \eta n$ AT HIGH ENERGY

The asymptotic behavior of hadronic cross sections is one of the important questions that NAL may be able to answer. We propose here a simple experiment to measure the $\pi^- p$ charge exchange cross section up to the highest energies available at NAL. This cross section is sensitive to small differences between the total cross section for $\pi^- p$ and $\pi^+ p$. If these cross sections persist in staying apart as is perhaps indicated by the Serpukhov data, then the charge exchange cross section will stay large.

In addition a measurement of $\pi^- p \to \eta^o n$ will be made. The $\pi^o$ reaction is a classic example in Regge theory of essentially pure $\rho$ exchange and the $\eta^o$ reaction of pure $A_2$ exchange. Thus this experiment will also test the predictions of this theory at high energies.

The experiment utilizes very simple equipment, but uses a new scheme to accurately determine the $\pi^o$ or $\eta^o$ direction. This is done by using a wire chamber to measure the $\gamma$-ray conversion points and a proportional wire chamber to identify which of the showers is most energetic. This knowledge allows one to uniquely solve for the direction of the $\pi^o$ or $\eta^o$ .

The experiment is planned to run at eight different energies between 20 and 200 GeV. The lower end will tie in to existing measurements. The time required is 400 hours including data taking and test time, in a $\pi^-$ beam with $\Delta p/p < \pm 0.5\%$, with intensity between $10^5$ and $5 \times 10^5$ $\pi^-$/pulse and with energy adjustable over the aforementioned range.

All of the necessary equipment, excluding the beam, but including the target, Cerenkov counters, shower counter, and fast electronics can be supplied by Caltech.

EXPERIMENTERS: A.V. Tollestrup, R.L. Walker
Caltech

CORRESPONDENT: A.V. Tollestrup

# I. PHYSICS JUSTIFICATION

We propose to measure the two reactions: 1) $\pi^- p \to \pi^0 n$ and 2) $\pi^- p \to \eta^0 n$ in the energy region between 20 GeV and 200 GeV and for momentum transfers between 0 and 2 GeV/$c^2$. The physics to be studied includes:

## A. Asymptotics

The recent results on meson-nucleon total cross sections at high energies[1] surprisingly show the measured $\pi^\pm$ cross sections constant above 30 BeV. The implications of these results are among the most exciting initial physics problems to pursue at NAL energies. The difference between the $\pi^+ p$ and $\pi^- p$ total cross sections does not appear to be asymptotically approaching zero.

The charge exchange cross section $\pi^- p \to \pi^0 n$ at $t = 0$ is sensitive to this difference in the $\pi^- p$ and $\pi^+ p$ total cross sections. We can write through the use of the optical theorem and charge independence the following equation:

$$\sigma_t(\pi^+ p) - \sigma_\tau(\pi^- p) = \frac{16}{S}\sqrt{2\pi}\ \mathrm{Im}\ \sigma_{\pi^- p \to \pi^0 n} \quad .$$

This means that a measurement of the charge exchange cross section is a sensitive way, in a single experiment, to obtain information on the asymptotic behavior of the difference of the $\pi^+$ and $\pi^-$ cross sections.

Appendix A of this proposal is a preprint of a paper by D. Horn and A. Yahil that explores in detail, by means of dispersion relations, what would happen if the $\pi^-$ and $\pi^+$ cross sections asymptotically approach a constant difference at high energies. It is seen from their Figure 4, which is reproduced on the next page, that the charge exchange cross section deviates from its 1/p

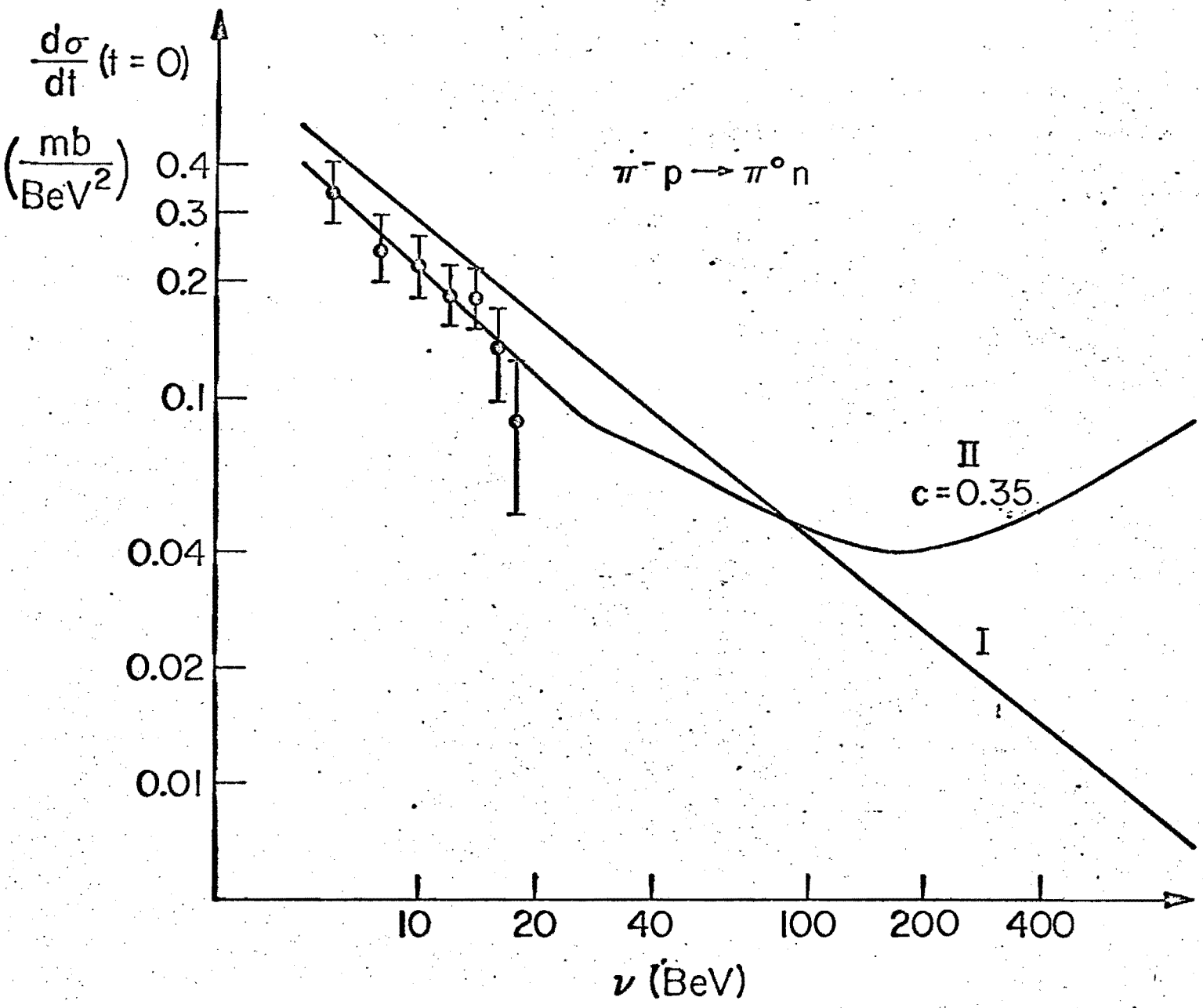


FIG. 4

FROM D. HORN
A. YAHIL
SEE APPENDIX A

dependence at low energies, to a flattening-off and subsequently an actual increase with rising energy.

B. Reggeizm.

The reactions to be measured in this experiment are dominated by a single exchange.

$$\pi^- p \to \pi^o n \qquad (\rho \text{ exchange})$$

$$\pi^- p \to \eta^o n \qquad (A_2 \text{ exchange})$$

They therefore represent an excellent place to study Regge theory as the energy of the process is increased. The highest energy measurements at present have only been made at 18 GeV.[3,5] The qualitative features of the data are a relatively sharp forward peak and a dip at $|t| \sim 0.6$ (GeV/c)$^2$ for $\pi^- p \to \pi^o n$. Will this behavior continue at higher energies? The dip is interpreted as resulting from the Regge trajectory $\alpha_\rho(t)$ going through zero near $-t \approx .6$. The $\pi^- p \to \pi^o n$ cross section has been the classic example for Regge theory. Excellent fits have been obtained from 2 GeV to 18 GeV. Originally pure $\rho$ exchange was tried and the complications of cuts in the angular momentum plane were ignored. However, the appearance of a small amount of polarization requires the presence of some other trajectory or cuts. Nevertheless, the fit to this reaction over such a wide energy range suggests this reaction as one to test the predictions of the Regge pole model as the energy is increased. Similar remarks can be made about the $\pi^- p \to \eta n$ cross section. Here the data has been fit by means of pure $A_2$ exchange. Again, the comparison of these fits at higher energy to actual measurements will provide an interesting test of Regge theory.

These two reactions in combination can be used to test certain predictions

of exchange degeneracy. $K^{o}p \to K^{+}n$, which is a combination of $\rho$ and $A_2$ exchange, must be exchange degenerate since it is an exotic channel and resonances are absent. The amplitude for this reaction, up to a phase, is identical to the line reversed reaction $K^{-}p \to \bar{K}^{o}n$.

The assumptions of exact SU(3) vertices plus exchange degeneracy leads to the sum rule

$$\frac{d\sigma}{dt}(K^{-}p \to \bar{K}^{o}n) = \frac{1}{2}\frac{d\sigma}{dt}(\pi^{-}p \to \pi^{o}n) + \frac{3}{2}\frac{d\sigma}{dt}(\pi^{-}p \to \eta^{o}n) \quad .$$

At 5.9 GeV/c, the data is consistent[6] with this sum rule for $\alpha(t) = 0.55 \pm 0.95t$. This experiment will yield some information on this sum rule at very different energies.

## II. EXPERIMENTAL DETAILS

### A. Introduction

This experiment is designed to measure the $\pi^o$ and $\eta^o$ cross sections in the range between 20 and 200 GeV.[1] The rough shape of the differential cross sections are shown below.

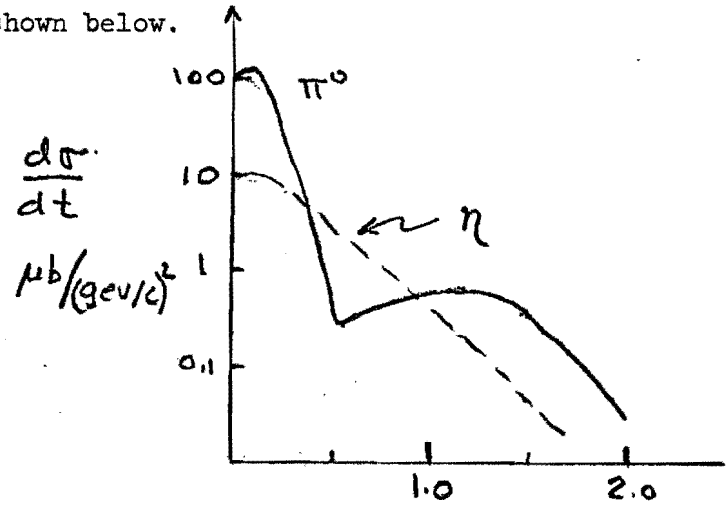


We have designed the equipment and selected the running time to give $10^4$ counts for $\pi^o$ production in the region of t less than 0.1 $GeV^2$ at each energy. This means that in the region of the second maximum the counting rate will be about 10 counts for a $\Delta t$ of 0.1. The resolution in t has been selected so that our minimum detectable t will be of the order of .002 and the accuracy on t in the whole range is better than .04. The experimental arrangement to accomplish this is fairly modest and is shown schematically in Figure 1. The $\pi^-$ enter the target, which is surrounded by a veto house to eliminate multi-pion reactions, and the $\pi^o$ is detected in the shower counter downstream. This technique has worked well at the lower energies at which this reaction has been measured and it will continue to work at these higher energies.[3,5]

In order to measure the value of t, one needs to know the incoming $\pi^-$

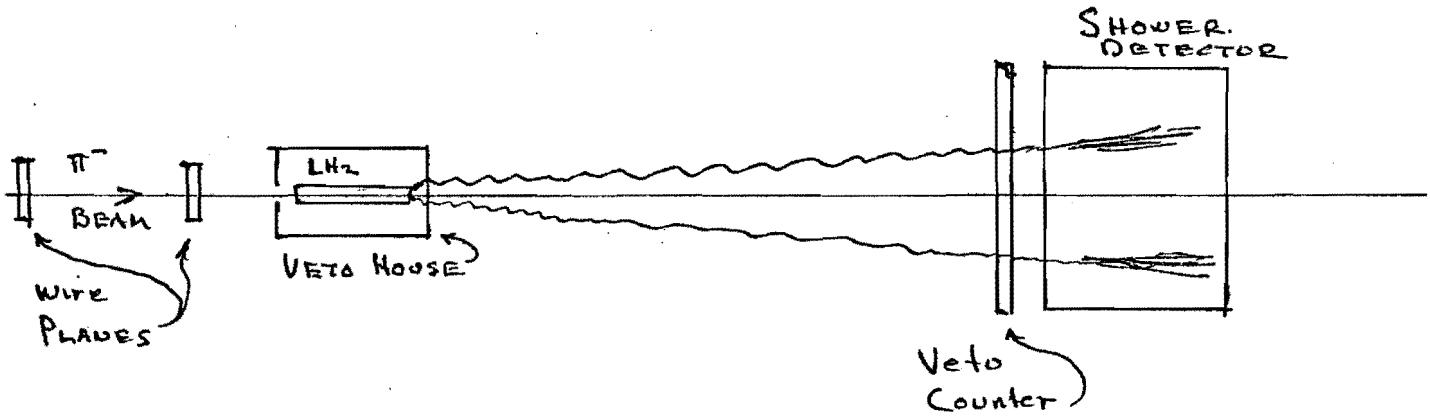
SHOWER
DETECTOR
$\pi^-$
BEAM
$LH_2$
VETO HOUSE
WIRE
PLANES
Veto
Counter

FIG. 1

direction and the outgoing $\pi^o$ direction very accurately, i.e., to less than 0.2 mr. Hence, there are proportional chambers in front of the target to measure the incoming $\pi^-$ direction and we describe in the section on the shower detector, how the angle of the $\pi^o$ is obtained to the required accuracy. The details of this equipment are described in the following sections.

B. Beam

The beam arrangement is shown in the following figure on a much exaggerated scale.

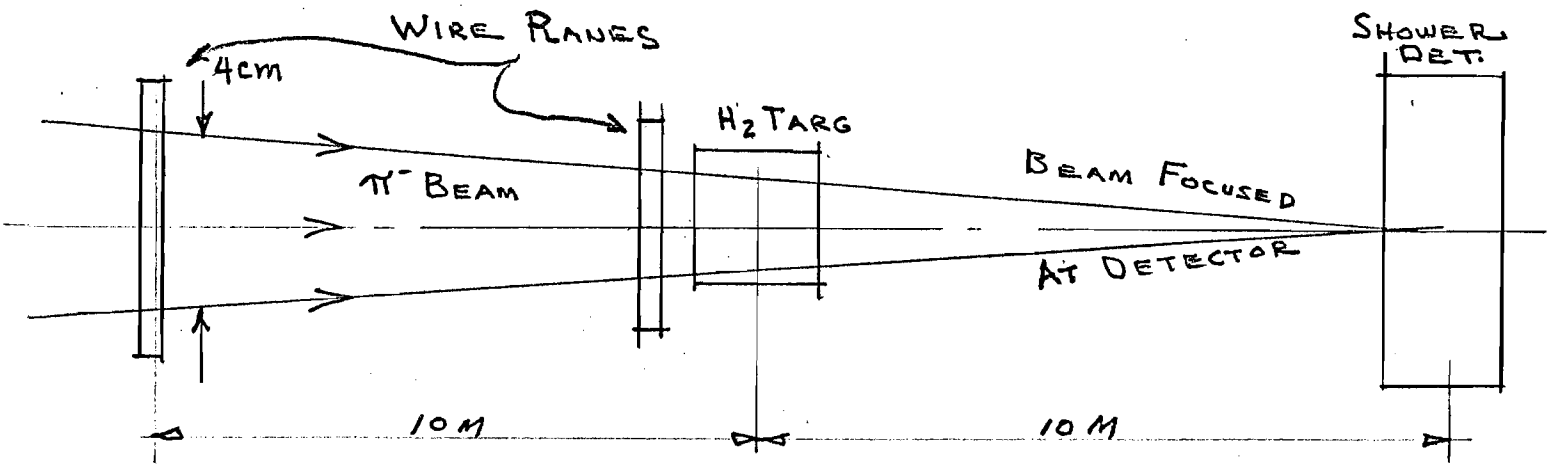


The parameters of the beam have been assumed to be those detailed by Reeder and MacLachlan.[4] The momentum resolution is not important and can be 1% or less. We have assumed the beam emittance to be 2 mr. x mm. As will be seen in the counting rate section, we can use an intensity of $10^5$ particles per pulse. As a rather large magnet would be required to deflect the beam off the detector, and as the intensity of the beam is rather low we have allowed the beam to hit the downstream detector. As shown in the drawing, the beam should be focussed at the detector where it will fall in a spot less than a millimeter in diameter. The detector can be deadened in this region if necessary. The size of the beam at

the target then becomes about 2 cm. and a target 2 feet long with a diameter of 2" would be an appropriate size for the experiment. To measure the incoming beam angle to an accuracy of 0.2 mr., we place a proportional chamber 3 cm. in diameter just in front of the target and a second proportional chamber 5 cm. in diameter 10 meters in front of the target. It is assumed that the beam particle position can be measured to 1 mm. in each one of these chambers giving an error on the incoming angle of .14 mr. A gas Cerenkov counter in front of the first proportional chamber identifies the incoming beam particle as a pion.

C. Target and Veto House

The target is a conventional hydrogen target 2 feet long with a cell about 2 in. in diameter. The surrounding jacket to the target should be kept as small as possible as it is necessary to build a veto house around the target. This veto house must be built carefully in order to veto efficiently multi-body reactions that occur within the target. It would consist of a layer of scintillator counters backed up by lead for converting gamma rays and an additional layer of scintillation counters.

The main source of background for a high energy forward pion will come from the diffractive processes which remain roughly constant with energy

$$\pi^- p \to \begin{matrix}(3\pi)\\(5\pi)\\\text{etc.}\end{matrix} + p \ .$$

For instance

$$\pi^- p \to A_1^- p$$

has a cross section roughly equal to 0.1 mb. and it is roughly independent of energy. If we assume 1 mb. cross section for all such processes, then the veto house must have a rejection of 500 to 1. We obtain this rejection by:

a) Demanding the $\pi^o$ have an energy $E_{\pi o} \geq 0.90\ E_{\pi -}$ . (Rejection assumed 1/10.)

b) Veto house efficiency for charged particles rejection 99%.

c) Single $\gamma$ veto efficiency $\geq 0.8$ .

These requirements taken together will provide sufficient rejection of the diffractive processes.

Non-diffractive processes all fall at least as fast as the charge exchange cross section with increasing energy and the requirements for good veto efficiency are easily met.

D. Detector

The forward $\pi^o$ detector is shown schematically below.

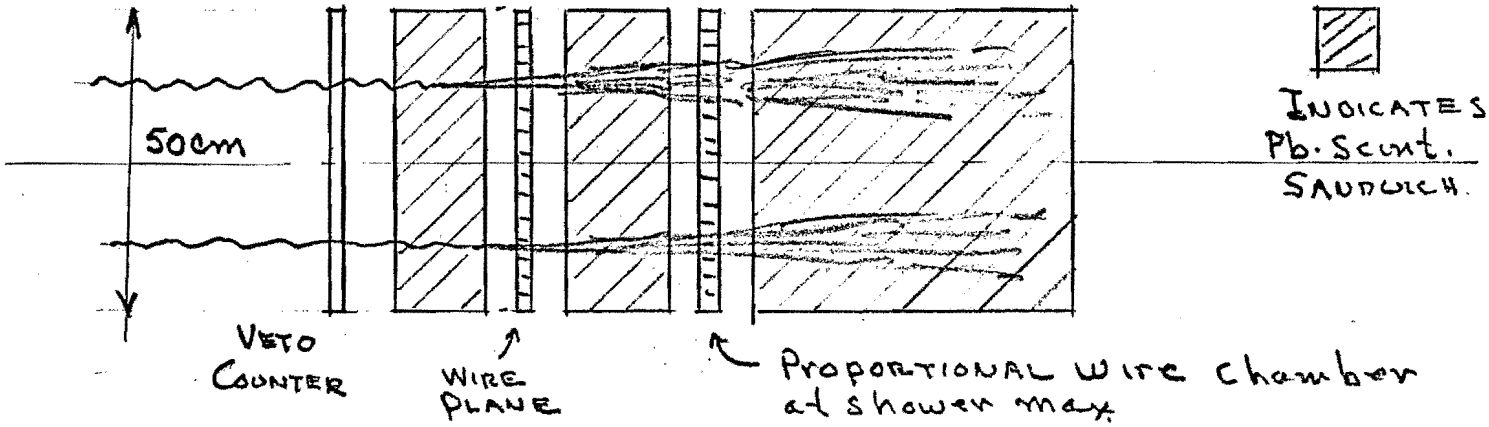


The veto counter insures that charged particles do not trigger the apparatus. The 2-$\gamma$ rays from the $\pi^o$ convert in the Pb-scintillator converter that is several

radiation lengths thick depending on the energy at which the experiment is being run. The wire plane measures the position of the two showers. This is then followed by a second Pb-scintillator sandwich whose pulse height when added to the converter section will determine the total $\gamma$-energy to $\Delta E/E < 5\%$. The wire chambers are triggered on the basis of this energy measurement provided none of the veto counters was triggered. The relative energy of the 2 showers is sampled by the proportional wire chamber which is located near shower maximum. This is used in a manner to be described shortly.

To get some idea of the problems involved, let's consider a 100 BeV $\pi^o$ generated in the target that decays symmetrically into two 50 BeV gamma rays which then strike the detector. The expression for half the opening angle is given by the following expression:

$$\theta_S = m_{\pi o}/E_{\pi o}$$

which is a small angle approximation. Two additional equations that are useful are the following:

$$E_1 = \frac{E_o}{(\theta_1/\theta_S)^2 + 1} \qquad \theta_1\,\theta_2 = \theta_S^2$$

where the meaning of the symbols is shown on the following figure:

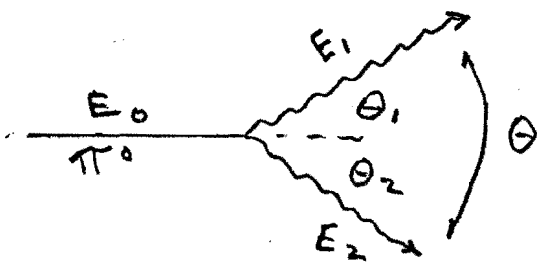


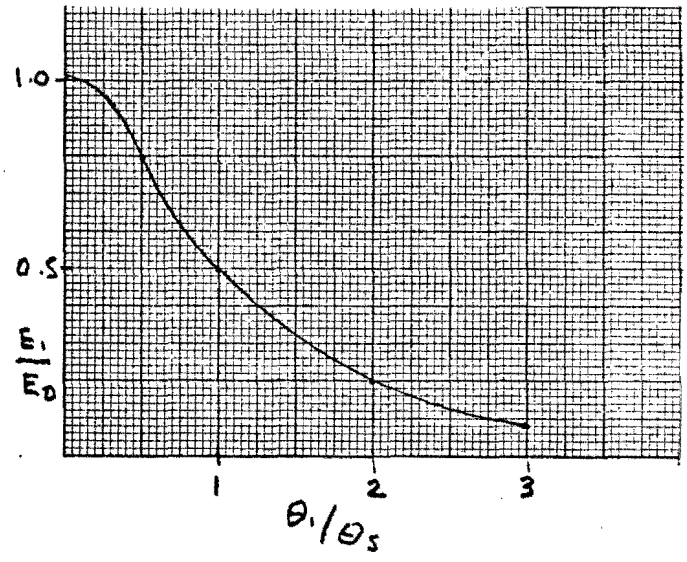

We see that for a 100 BeV $\pi^o$ that $\theta_s = 1.4$ mr. That means that at the detector, the two showers in the symmetrical case are separated by 2.8 cm. In the case of asymmetrical decay the separation is greater and the energies are no longer equal, as can be seen in the above figure. Now it is clear that if we measure the distance between the two showers, that this does not allow us to uniquely define the $\pi^o$ direction. In fact,we have

$$\theta = \theta_1 + \theta_2$$

where $\theta$ is the opening angle of the pair. We can combine this equation with the following one:

$$\theta_1 \, \theta_2 = \theta_s^2$$

and we see that there is a two-fold ambiguity in the direction of the $\pi^o$ .

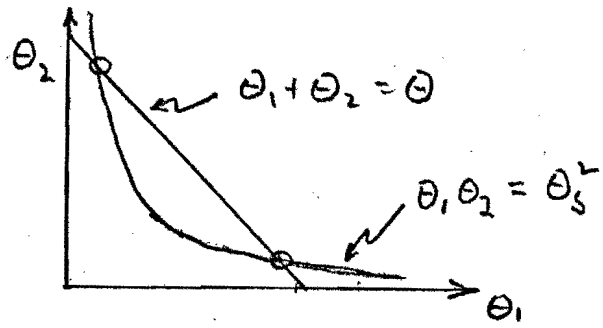


This leads to an uncertainty in the t of the reaction that is unacceptable. However, if we can arrange in the detector to identify which gamma ray has the highest energy, we can resolve this two-fold ambiguity. The detector is therefore constructed to make a rough energy measurement of the individual showers.

From the figure above that indicates how the energy of the gamma ray varies with angle we see that we only need a rather crude energy measurement in order to tell the two gamma rays apart, except in the region around $\theta_s$ . In this region the two gamma rays have nearly the same energy and a detector with poor resolution may not be able to resolve them. On the other hand, in this region if one

assumes that the $\pi^o$ direction bisects the two showers, the error on the momentum transfer is very small anyway. A detailed examination shows that if we can make an energy measurement of the individual gamma rays to 30%, that the perpendicular momentum transmitted to the nucleon is then never uncertain by more than 40 MeV. It is for this reason that we insert a proportional wire chamber in the converters near where the shower maximum should occur. For instance, a 50 BeV shower has its maximum at about 8 radiation lengths. There are about 200 electrons in the core which is about 1 cm. in diameter.

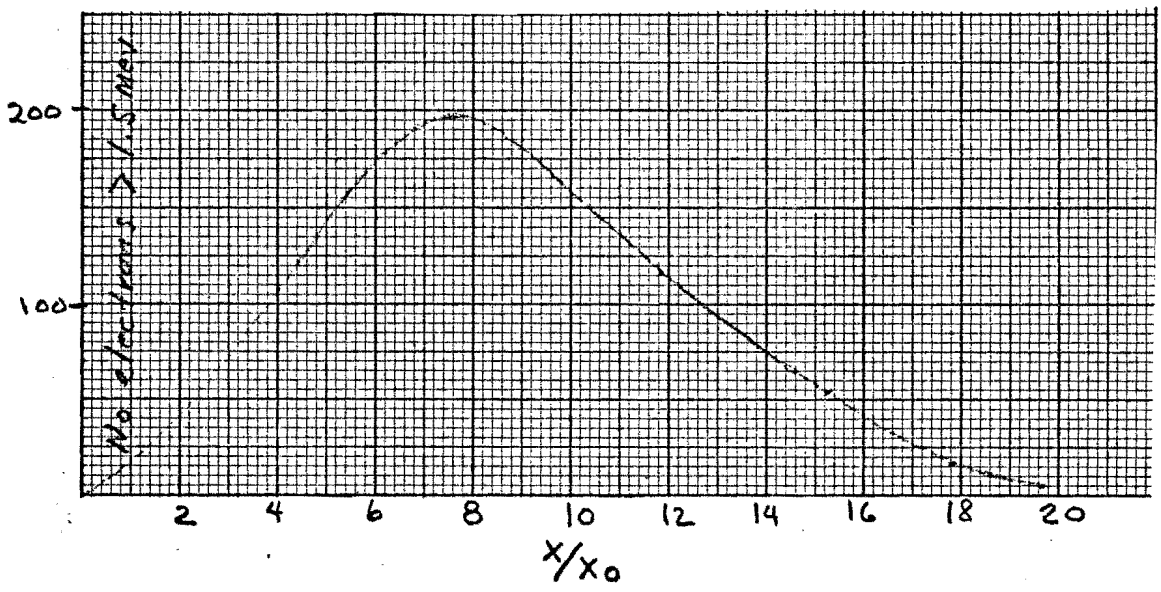


The two showers from a 100 BeV $\pi^o$ will be separated by 2.8 cm. or more and hence do not overlap seriously. The total ionization at shower maximum is proportional to the $\gamma$-ray energy and will be recorded for each shower by the proportional chamber and used to identify the higher energy one. It should be noted that a crossed counter hodoscope made up of 1 cm. wide counters could be used in the same way. The ionization loss is so large that cheap ½" diameter photomultipliers could be used.

E. Counting Rate

Sondereger[3] gives the following expression for the $\pi^o$ reaction:

$$\sigma(t < 0.5) = 720\ \mu b/p^{1.17} \quad .$$

This was measured over the energy region from 6 to 18 GeV and of course the extrapolation to 150 GeV is somewhat uncertain. However, we have used the above equation to estimate the counting rates which are shown in the following table.

| | $\pi^- p \to \pi^o n$ | | | $\pi^- p \to \eta n$ | | |
|---|---|---|---|---|---|---|
| p | $\sigma_{t<0.5}$ μb | $\frac{d\sigma}{dt}\ t = 0$ | Counts/hr. $t < 0.1$ | $\sigma_t$ | $\frac{d\sigma}{dt}\ t = 0$ | Counts/hr. all t |
| 20 | 21 | 110 | 1550 | 33 | 140 | 4600 |
| 40 | 9.6 | 60 | 840 | 13 | 56 | 1700 |
| 60 | 6 | 38 | 530 | 7 | 10 | 1000 |
| 80 | 4.2 | 30 | 420 | 5 | 2 | 700 |
| 100 | 3.3 | 23 | 320 | 3.5 | 1.5 | 500 |
| 120 | 2.7 | 20 | 280 | 2.7 | 1.2 | 380 |
| 140 | 2.2 | 16 | 225 | 2.2 | 1.0 | 320 |
| 200 | 1.4 | 12 | 170 | 1.3 | 0.6 | 180 |

Table assumes:

a) $\sigma_{t<0.5} = \left(720\right)/p^{1.17}$ $\quad \pi^- p \to \pi^o n$ $\quad$ (p in gev/c)

b) $d\sigma/dt\Big)_{t=0} = \frac{2200}{p}$ $\quad \pi^- p \to \pi^o n$

c) $10^5$ π/pulse 700 pulses/hr.

d) 2' long $H_2$ target.

e) $d\sigma/dt\Big)_{t=0} = \left(\frac{100}{P_{gev}}\right)^{1.4}$ μb for $\pi^- p \to \eta^o n$

We have made a similar extrapolation of the data of O. Guisan et al.[5] for the $\eta^o$ cross section, and the results of that extrapolation are also shown in the above table. In order to accumulate at the energies shown above $10^4$ counts for t less than 0.1 GeV we will need 250 hours of running time. In order to check out the equipment and the beam, we estimate that we will need an additional 150 hours. Therefore we request a total running time of 400 hours.

F. Equipment

1) Beam: beam Cerenkov counter to distinguish $\pi$ from $K^-$ and $\bar{p}$ ; 2 proportional wire chambers, about 5 cm. x 5 cm.

2) Target: 2 foot hydrogen target, 2 in. in diameter, constructed in a fashion suitable for placing veto counters around it.

3) Detector: 2 wire planes; a proportional chamber; and associated scintillation counters for measuring the shower properties.

4) Electronics: PDP-8 computer for recording the data; wire chamber readout; and miscellaneous fast electronics.

5) Miscellaneous equipment: 2 graduate students; 2 undergraduate students; R.L. Walker has indicated he wishes to also be listed here.

All of the above equipment, including the target, could be furnished by Caltech and be ready to operate by the time the accelerator can provide a beam.

REFERENCES

(1) IHEP-CERN Collaboration, J.V. Allaby et al., Physics Letters 30B, 500 (1969).

(2) This reaction was studied by J. Kirz in NAL Summer 1969 Study, Vol. 4, pp. 71-75.

(3) A.V. Stirling, P. Sonderegger, J. Kirz, P. Falk-Vairant, O. Guisan, C. Bruneton, P. Borgeaud, M. Yvert, J.P. Guillaud, C. Caverzasio, B. Amblard, PRL 14, 763 (1965).

(4) D. Reeder and J. MacLachlan, NAL 1969 Summer Study, Vol. 1, pp. 41-53.

(5) O. Guisan, J. Kirz, P. Sonderegger, A.V. Stirling, P. Borgeaud, C. Bruneton, P. Falk-Vairand, A. Amblard, C. Caversasio, J.P. Guillaud, M. Yvert, Physics Letters 30B, 500 (1969).

(6) The best discussion of this problem is given by R.D. Mathews, Nuc. Phys. B11, 339 (1969).

# APPENDIX A

to be submitted to Physical Review.

CALT-68-238

AEC RESEARCH AND
DEVELOPMENT REPORT

# Real Parts of Meson-Nucleon Forward Scattering Amplitudes*

D. HORN** and A. YAHIL

California Institute of Technology, Pasadena, California 91109

(Received January , 1970)

## ABSTRACT

A dispersion relation calculation of the real parts of forward $\pi^{\pm}p$ and $K^{\pm}p$ scattering amplitudes is carried out under the assumption of constant total cross sections in the Serpukhov energy range. Comparison with existing experimental results as well as predictions for future high energy experiments are presented and discussed. Electromagnetic effects are found to be too small to account for the expected difference between the $\pi^-p$ and $\pi^+p$ total cross sections at higher energies.

*Work supported in part by the U. S. Atomic Energy Commission. Prepared under Contract AT(11-1)-68 for the San Francisco Operations Office, U. S. Atomic Energy Commission.

**On leave of absence from Tel Aviv University, Tel Aviv, Israel.

## I. INTRODUCTION

The recent Serpukhov experiments[1] show that all measured meson-nucleon total cross sections stay constant at energies above 30 BeV. This contradicts previous expectations from theories describing the behavior of the cross sections at energies below 30 BeV. In the present paper, we investigate the effect of the new results on the real parts of meson-nucleon scattering amplitudes via dispersion relations. We analyze the $\pi^{\pm}p$ system following the approach developed in Ref. 2. We discuss the phase of the forward $\pi^{\pm}p$ scattering amplitudes as well as the forward differential cross section of $\pi N$ charge exchange (CEX). We find an estimate for the upper limit of electromagnetic effects in these amplitudes, and conclude that it is too small to account for the expected difference between $\sigma_T(\pi^-p)$ and $\sigma_T(\pi^+p)$ at the higher energies. We discuss the fits to presently available data and make predictions for future high-energy experiments. We treat $K^{\pm}p$ scattering in a similar way. Although the experimental data on the real parts of the amplitudes are not very accurate, they favor the existence of an additional term. This would be implied if the difference between $\sigma_T(K^-p)$ and $\sigma_T(K^+p)$ persists at higher energies.

It should be noted that in order to evaluate the real part, it is only necessary to speculate on the behavior of the total cross sections up to energies which are, say, an order of magnitude greater. A different extrapolation beyond there does not necessarily affect the dispersion calculation.

In Section II we present the general formalism and discuss a mathematical example that is close to the real situation in $K^{\pm}p$. In Section III we treat the $\pi p$ problem in detail. Section IV deals with the $Kp$ system.

## II. GENERAL FORMALISM

We use dispersion relations to analyze a $t = 0$ scattering amplitude, whose discontinuity is determined by total cross sections of two channels related by crossing (e.g., $\pi^+p$ and $\pi^-p$ or $K^+p$ and $K^-p$). We refer the reader to Ref. 3 for the conventional formulation of dispersion relations and previous calculations. One separates the symmetric amplitude $A^{(+)} = \frac{1}{2}\left[A(\pi^-p) + A(\pi^+p)\right]$ from the antisymmetric one $A^{(-)} = \frac{1}{2}\left[A(\pi^-p) - A(\pi^+p)\right]$, and writes the dispersion relations

$$A^{(+)}(\nu) = A^{(+)}(\mu) + \frac{f^2 k^2}{M\left[1 - \left(\frac{\mu}{2M}\right)^2\right]\left[\nu^2 - \left(\frac{\mu^2}{2M}\right)^2\right]} + \frac{k^2}{2\pi^2}\int_\mu^\infty d\nu' \, \frac{\nu' \, \sigma^{(+)}(\nu')}{k' \, (\nu'^2 - \nu^2 - i\epsilon)} \quad , \tag{1}$$

$$A^{(-)}(\nu) = \frac{2f^2 \nu}{\nu^2 - \left(\frac{\mu^2}{2M}\right)^2} + \frac{\nu}{2\pi^2}\int_\mu^\infty d\nu' \, \frac{k' \, \sigma^{(-)}(\nu')}{\nu'^2 - \nu^2 - i\epsilon} \quad . \tag{2}$$

M is the nucleon mass and $\mu$ the meson mass. $\sigma^{(\pm)} = \frac{1}{2}\left[\sigma_T(\pi^-p) \pm \sigma_T(\pi^+p)\right]$. $\nu$ and k are the meson's laboratory energy and momentum respectively. $f^2$ specifies the strength of the Born term, and is equal to 0.082. $A^{(+)}(\nu = \mu)$ is the only subtraction constant. It is known to be zero within experimental errors, in agreement with Adler's PCAC self-consistency condition.[4] In writing (2), one obviously makes the assumption that $\sigma^{(-)}$ goes asymptotically to zero. This is the point which we now want to change. Following the approach of Ref. 2, we assume that both $\sigma_T(\pi^-p)$ and $\sigma_T(\pi^+p)$ remain constant from about 30 BeV on. This then implies that they have different values, and $\sigma^{(-)}$ is a non-zero constant. We want to

see what the predictions of these assumptions for the real part are. Having to introduce a subtraction into (2), we therefore replace it by

$$A^{(-)}(\nu) = \frac{2 f^2 \nu}{\nu^2 - (\frac{\mu^2}{2M})^2} + \frac{\nu}{2\pi^2} \int_{\mu}^{\kappa} d\nu' \frac{k' \sigma^{(-)}(\nu')}{\nu'^2 - \nu^2 - i\epsilon}$$

$$+ \frac{\nu k^2}{2\pi^2} \int_{\kappa}^{\infty} d\nu' \frac{\sigma^{(-)}(\nu')}{k' (\nu'^2 - \nu^2 - i\epsilon)} + c \frac{\nu}{M^2} \quad . \qquad (3)$$

Note that, instead of performing a subtraction on the entire integral, we divide it into two parts. One is written in an unsubtracted form, and the other in a subtracted one. This is done for practical purposes. It avoids stressing the low-energy input and thus increasing the errors in the calculation. The number c depends on the choice of $\kappa$. Equation (3) also demonstrates the fact that the real part at low energy is not necessarily affected by the new assumptions on the high-energy behavior. We are actually able to reproduce at low energies (say, below 4 BeV) the same results previously obtained by the use of (2) with any reasonably decreasing fit to $\sigma^{(-)}$.

To illustrate the changes brought about by the assumptions on the behavior of the total cross section, let us discuss a mathematical example that is very similar to the actual situation in $K^{\pm}p$. Let us denote the two reactions in question by A and B (analogous to $K^+p$ and $K^-p$ respectively). Assume first that (case I):

$$\text{Im } A_I = a\,\nu \quad , \quad \text{Im } B_I = a\,\nu + b\sqrt{\nu} \quad , \quad 0 < \nu < \infty \quad . \qquad (4)$$

It is then easy to find that

$$\text{Re } A_I = -\,b\sqrt{\nu} \quad , \quad \text{Re } B_I = 0 \quad . \qquad (5)$$

This is the expected result for $K^{\pm}p$ if one uses a Regge representation with a regular Pomeron and two pairs of exchange degenerate trajectories with intercepts at 1/2. If we now make the analogous assumption to that of Ref. 2, we have (case II):

$$\text{Im } A_{II} = a\,\nu \quad , \qquad \text{Im } B_{II} = \begin{cases} a\,\nu + b\,\sqrt{\nu} & 0 < \nu < \Lambda \\ (a + \frac{b}{\sqrt{\Lambda}})\,\nu & \Lambda < \nu < \infty \end{cases} \quad . \tag{6}$$

It is then readily established that

$$\begin{aligned} \text{Re } A_{II} &= -\frac{2b\sqrt{\nu}}{\pi} \arctan\sqrt{\frac{\Lambda}{\nu}} + \frac{b\,\nu}{\pi\sqrt{\Lambda}} \log|\nu+\Lambda| - \frac{c}{M^2}\,\nu \quad , \\ \text{Re } B_{II} &= \frac{b\sqrt{\nu}}{\pi} \log\left|\frac{\sqrt{\nu}-\sqrt{\Lambda}}{\sqrt{\nu}+\sqrt{\Lambda}}\right| - \frac{b\,\nu}{\pi\sqrt{\Lambda}} \log|\nu-\Lambda| + \frac{c}{M^2}\,\nu \quad . \end{aligned} \tag{7}$$

It is now interesting to note that although Eqs. (5) and (7) are very different from one another, it is still possible to find a value of c that will show a similar behavior for low $\nu$. Thus it is possible that even though $\text{Im } B_I \neq \text{Im } B_{II}$ for $\nu > \Lambda$, one still finds that the real parts of the various amplitudes can roughly agree for $\nu < \Lambda$.

To illustrate this point numerically, we choose $a = b = 3.6$, $\Lambda = 22$. (These values are indicated by experiment if $\nu$ is measured in BeV and the amplitudes in $\text{BeV}^{-1}$.) We find such an agreement between I and II for $c = 1.1$. We present in Fig. 1 the results for $\alpha(A) = \text{Re } A/\text{Im } A$ and $\alpha(B) = \text{Re } B/\text{Im } B$, since this is the customary way in which the data are given in $\pi N$ experiments.

Note that after the value $\nu \simeq 100$ the logarithmic part in $\text{Re } A_{II}$ and $\text{Re } B_{II}$ is taking over. Nevertheless it does not reach a sizable amount even at high $\nu$ values. To quote a number -- at $\nu = 10^6$ we find

$\alpha(B_{II}) = -0.49$ and $\alpha(A_{II}) = 0.59$. We will find a similar behavior in the next section when discussing the $\pi N$ problem.

## III. REAL PARTS OF $\pi^{\pm}p$ AMPLITUDES

In Ref. 2, the $\pi^{\pm}p$ total cross sections were fitted to a form

$$\sigma_{\pm} = a_{\pm} + b_{\pm}/\sqrt{\nu} \quad . \tag{8}$$

An ionization point was then assumed to appear at $\nu = 30$ BeV, resulting in the flattening off of the cross sections at that point. This meant that $2\sigma^{(-)} = \sigma(\pi^-p) - \sigma(\pi^+p) > 1$ mb even at high energies. In Ref. 2, $\sigma^{(-)}$ was assumed to remain a constant for $\nu \geq 30$ BeV.

Any breaking of the Pomeranchuk theorem results in a logarithmic rise of the real part of the amplitude, notably of $A^{(-)}(\nu)$.[2,5] Hence $\alpha_{\pm}(\nu) = \text{Re } A_{\pm}(\nu)/\text{Im } A_{\pm}(\nu)$ does not tend to 0 as $\nu \to \infty$. Once the logarithmic behavior begins to dominate, $\alpha$ rises in absolute value, with $\alpha_+$ and $\alpha_-$ taking opposite signs. The strength of the logarithmic term is proportional to the value of $\sigma^{(-)}$.

The dispersion integrals were evaluated on a computer. In order to do the principal part integration, it is necessary to have a smooth fit to the data points, since the integral is sensitive to discontinuities near $\nu' = \nu$. For $\nu \leq 4$ BeV we used the fit of Ref. 3. The data between 4 and 30 BeV[6,7] can be fitted in a variety of ways. We first fitted each cross section separately to a form

$$\sigma_{\pm} = a_{\pm} + b_{\pm}\, \nu^{n-1} \quad . \tag{9}$$

In such fits, $a_- - a_+$ was invariably greater than 1 mb, and the choice of n was a matter of taste. We then tried a fit satisfying the Pomeranchuk theorem

$$\sigma_{\pm} = a + b\,\nu^{n-1} \pm c\,\nu^{m-1} \quad . \qquad (10)$$

This was done in order to be able to compare the premise of a cutoff with the assumption that the Serpukhov data might be wrong, and that the Pomeranchuk theorem might be right after all.

The data of Citron et al.[6] do not seem to fit smoothly to those of Foley et al.[7]. We had to settle for a slightly low value of n. We chose

$$n = 0.25 \quad , \quad m = 0.6 \quad .$$

Applying to fit (10) a cutoff at 30 BeV, we got for $\nu$ above cutoff

$$2\sigma^{(-)} = \sigma(\pi^- p) - \sigma(\pi^+ p) = 1.3 \text{ mb} \quad .$$

This number is consistent with the result of Ref. 1. In doing the same with fit (9), we got $2\sigma^{(-)}$ above cutoff to depend on the fit. $\sigma(\pi^- p)$ is, of course, determined by the Serpukhov data, but there is a slight freedom of play in $\sigma(\pi^+ p)$. We assumed the cutoff point to be the same as in $\pi^- p$ (30 BeV) and since this is 8 BeV higher than the last data point, the extrapolation depends on the fit. If we constrained fit (9) to satisfy $2\sigma^{(-)} = 1.3$ mb, the dispersion relations gave the same results for the real parts as fit (10). We adopted the latter for the purpose of testing the sensitivity of the calculation to the possible breaking of the Pomeranchuk theorem. We called case I that which assumes (10) to be good for all $\nu$. In case II we applied the cutoff, so that for $\nu \geq 30$ BeV both cross sections were constant. The two cases are illustrated in Fig. 2. Note that if further structure appears in $\sigma_T$ at much higher energies, it may have negligible effects on our calculation.

The calculated ratios $\alpha_{\pm}(\nu) = \text{Re } A_{\pm}(\nu)/\text{Im } A_{\pm}(\nu)$ for the $\pi^{\pm} p$ amplitudes are plotted in Fig. 3, together with the data.[8] In case I there

is no free parameter in the dispersion relations (1) and (2). In case II there is the arbitrariness of c in (3), which can be chosen to best fit the data. (We used $\kappa = 4$ BeV.)

If one assumes exact charge independence, one can evaluate the forward CEX differential cross section. The predictions are plotted together with the data[9] in Fig. 4 and Fig. 5. We note that in case I the prediction seems to be too high by about 30% at, say, 20 BeV. If we attribute the discrepancy to I-spin violation of the electromagnetic amplitude, we find it to be 20% of the total $A^{(-)}$ amplitude. With $2\sigma^{(-)}(\nu=20) \sim 1.5$ mb, we would thus have $2\sigma_{EM}^{(-)} \lesssim 0.3$ mb. Since we do not expect the electromagnetic effects to vary strongly with energy, we may conclude that the ansatz of the Pomeranchuk theorem is good only up to $2\sigma^{(-)}(\infty) \lesssim 0.3$ mb.

In case II one can adjust c so as to get a very good fit to the CEX data ($c = 0.35$). Alternatively, one can fix c to fit the $\alpha_\pm$ data. Choosing here $c = 0.35$, we find a good fit to $\alpha_+$ but a poor one to $\alpha_-$. This is an improvement over case I. A change to $c = 0.25$ results in an equivalent overall fit to $\alpha_\pm$ with a poorer fit to $\alpha_+$ and a better one to $\alpha_-$. Note that such a change contributes oppositely to $\alpha_+$ and $\alpha_-$. Checking the CEX prediction with $c = 0.25$, we find it too low by about 40%. This corresponds to $2\sigma_{EM}^{(-)} \lesssim 0.5$ mb.

Note that the small deviations that we found are a feature of our calculated real parts. Point by point, the experimental $\alpha_\pm(\nu)$, within their errors, are consistent with the CEX data without any I-spin violation. This was already pointed out by Foley et al.[8] Although we can fit the data with no I-spin breaking, we cannot rule out $2\sigma_{EM}^{(-)} \lesssim 0.5$ mb. However, this is still too small to account for the expected constant difference between $\sigma_T(\pi^- p)$ and $\sigma_T(\pi^+ p)$. We have to conclude, then, that this difference is a genuine strong interaction effect.

The main difference between the two dispersion calculations I and II sets in around 100 BeV. At that point, the logarithmic part of Re $A^{(-)}$ in case II begins to dominate. Instead of going to zero, $\alpha_+(\nu)$ becomes positive and increases, while $\alpha_-(\nu)$ turns over and becomes more negative. The CEX forward cross section begins to rise again. On an absolute scale, both effects are small. We should be able to see the CEX forward cross section flattening, but for the real part to dominate the amplitude we will need fantastically high energies. By that time, a new physics may very well set in. It was pointed out in Ref. 2, as well as in Ref. 5, that if Re A/Im A grows logarithmically, then one has to have the forward elastic peak shrink like $\log^2 s$ to avoid a conflict with unitarity. Strictly speaking, such a conflict would arise only at such large values of $\nu$ that the whole problem looks rather academic. Nevertheless, the same conclusion about the shrinkage arises of course from the assumption that $\sigma_{el}$ does not rise with energy, which might very well be the case.

Finally, a word about errors and low-energy behavior. The cross sections are accurate to about 1%. This leads to errors of approximately $\pm 0.003$ in $\alpha_\pm(\nu)$. A change in $\sigma^{(-)}$ above cutoff causes a bigger correction. Varying the high-energy cross sections above 30 BeV does not change the low-energy ($\nu \leq 4$ BeV) dispersion calculations. There, our results agree with those of Ref. 3.

## IV. REAL PARTS OF $K^\pm p$ AMPLITUDES

We calculated the real parts of $K^\pm p$ forward scattering amplitudes in the same way as for $\pi^\pm p$. The data between threshold and $\nu = 3.3$ BeV were slightly smoothed. Above that point, the following fit was made:

$$\sigma(K^+p) = a \quad ,$$
$$\sigma(K^-p) = a + b/\sqrt{\nu} \quad . \tag{11}$$

The dispersion relations were evaluated for cases I and II as in $\pi p$, with the cutoff in case II taken at 20 BeV. The errors involved here are much bigger than in $\pi p$. The uncertainties in the subthreshold singularities do not allow a good determination of the real parts at low energies. In particular, the $Y^*(1405)$ is an S-wave, and thus is not quenched kinematically. We estimate its effect to be six times as big as the Born term in $\pi N$. This would be approximately 5 - 10% of the real part at $\nu = 5$ BeV. An additional unknown is the subtraction term of the symmetric amplitude, $A^{(+)}(\nu=\mu)$. However, their combined effect remains constant, while the imaginary part grows like $\nu$, so that their contribution to $\alpha(K^{\pm}p)$ should fall like $1/\nu$. In case II there is the further difficulty of evaluating the subtraction constant c in the antisymmetric amplitude $A^{(-)}$. The CEX reactions are not related by a simple I-spin rotation. Nor has a direct experimental determination of $\alpha_{\pm}(\nu)$ by Coulomb interference been done. The only existing test is the forward elastic differential cross section. This is a measurement of $1 + \alpha^2$. If $\alpha$ is small, its determination becomes difficult. Fortunately there exists relatively accurate $K^+p$ data,[10] which suggests $|\alpha(K^+p)| \sim 0.55 \pm 0.15$ for $\nu \sim 7 - 15$ BeV. The error in $\alpha$ is evaluated by assuming the $d\sigma/dt$ data to vary within their error bars. If we allow a further variation of one standard deviation, we can set a lower limit on $\alpha$ of $\sim 0.25$. The $K^-p$ data[11] is consistent with $|\alpha(K^-p)| = 0$, but an upper limit of $\sim 0.3$ has to be allowed within error bars. An additional standard deviation increases this limit to $\sim 0.5$. The

calculated values of $\alpha(K^{\pm}p)$, together with the experimental limits are plotted in Fig. 6.

Case I seems to disagree with the data. In case II we can explain the discrepancy by means of the subtraction term. To fit $\alpha(K^{+}p)$, we can choose either one of two values, depending on the sign of $\alpha$, which cannot be determined by this method. We find for $\kappa = 3.3$,

$$c = \begin{cases} 2 & \alpha(K^{+}p) < 0 \quad , \quad \alpha(K^{-}p) > 0 \\ -1.6 & \alpha(K^{+}p) > 0 \quad , \quad \alpha(K^{-}p) < 0 \end{cases} .$$

$c = -1.6$ is ruled out because it gives $\alpha(K^{-}p) \sim -0.65$. Hence we conclude that $\alpha(K^{+}p) < 0$ and $\alpha(K^{-}p) > 0$. The data points for $\alpha(K^{+}p)$ were plotted under this assumption in Fig. 6. The errors are clearly very large, and allow us to safely ignore the subthreshold singularities.

The general features of $\pi p$ dispersion relations appear also in $Kp$. The logarithmic behavior is magnified because $2\sigma^{(-)} \sim 4$ mb. However, at present energies the bulk of the real part seems to come from the subtraction term, and not from the logarithmic one. In fact, these appear to have opposite signs. Thus we expect $|\alpha|$ to actually fall until very high energies, when $\alpha$ changes signs and $|\alpha|$ begins to grow again. As in $\pi p$, the real part does not dominate until extremely high energies.

The difference between the pion and the kaon amplitudes lies in the energy range below the cutoff point. The usual Regge picture -- which assumes the Pomeranchuk theorem to hold -- is compatible with experiment for the pions, but appears not to be so for the kaons. In the latter case, the existence of an additional real term seems to be implied by the data.

## REFERENCES


1. IHEP-CERN Collaboration, J. V. Allaby et al., Physics Letters 30B, 500 (1969).
2. D. Horn, Caltech report CALT-68-228 (to be published).
3. G. Höhler, G. Ebel, and J. Giesecke, Zeit. f. Physik 180, 430 (1964).
4. S. L. Adler, Phys. Rev. 139, B1638 (1965).
5. R. J. Eden, University of California at Riverside report UCR-34P107-105 (1969).
6. A. Citron et al., Phys. Rev. 144, 1101 (1966). (This data was later revised. See G. Giacomelli et al., Hera Group Compilation, CERN report CERN/HERA 69-1.)
7. K. J. Foley et al., Phys. Rev. Letters 19, 330 (1967).
8. K. J. Foley et al., Phys. Rev. 181, 1775 (1969).
9. I. Mannelli et al., Phys. Rev. Letters 14, 408 (1965).
10. K. J. Foley et al., Phys. Rev. Letters 11, 503 (1963); C. Y. Chien et al., Physics Letters 28B, 615 (1969). We use the fit of the Particle Data Group, L. R. Price et al., UCRL 20000 $K^+N$ (September 1969).
11. K. J. Foley et al., Phys. Rev. Letters 15, 45 (1965); M. Aderholz et al., Physics Letters 24B, 434 (1967).

## FIGURE CAPTIONS

Fig. 1: $\alpha$, the ratio of real and imaginary parts of the various amplitudes discussed in the mathematical example of Section II. The subtraction constant c is chosen so that for $\nu < \Lambda$, $\alpha_I \approx \alpha_{II}$.

Fig. 2: $\pi^{\pm}p$ total cross sections and fit (10). Errors plotted are the sum of the statistical and the systematic. The statistical errors of Allaby et al. are also indicated. The errors of Citron et al. are mainly systematic, and only representative data points of this group have been included.

Fig. 3: Predicted $\alpha(\pi^{\pm}p) = \text{Re } A(\pi^{\pm}p)/\text{Im } A(\pi^{\pm}p)$ and experimental data of Foley et al.[8] I and II refer to the choice of high-energy cross sections. (See Fig. 2.) c is the subtraction constant.

Fig. 4: Forward differential $\pi N$ charge exchange cross sections predicted assuming exact I spin conservation, and data of Mannelli et al.[9]

Fig. 5: Blow-up of Fig. 4. The discrepancy between the fit and the data is an indication of the amount of I-spin violating electromagnetic effect. On the basis of this deviation, we conclude $2\sigma_{EM}^{(-)} \lesssim 0.5$ mb.

Fig. 6: $\alpha(K^{\pm}p) = \text{Re } A(K^{\pm}p)/\text{Im } A(K^{\pm}p)$ and experimental limits deduced from the forward elastic differential cross sections.[10,11] The sign of $\alpha(K^{+}p)$ was determined from the dispersion relations. (See text.)

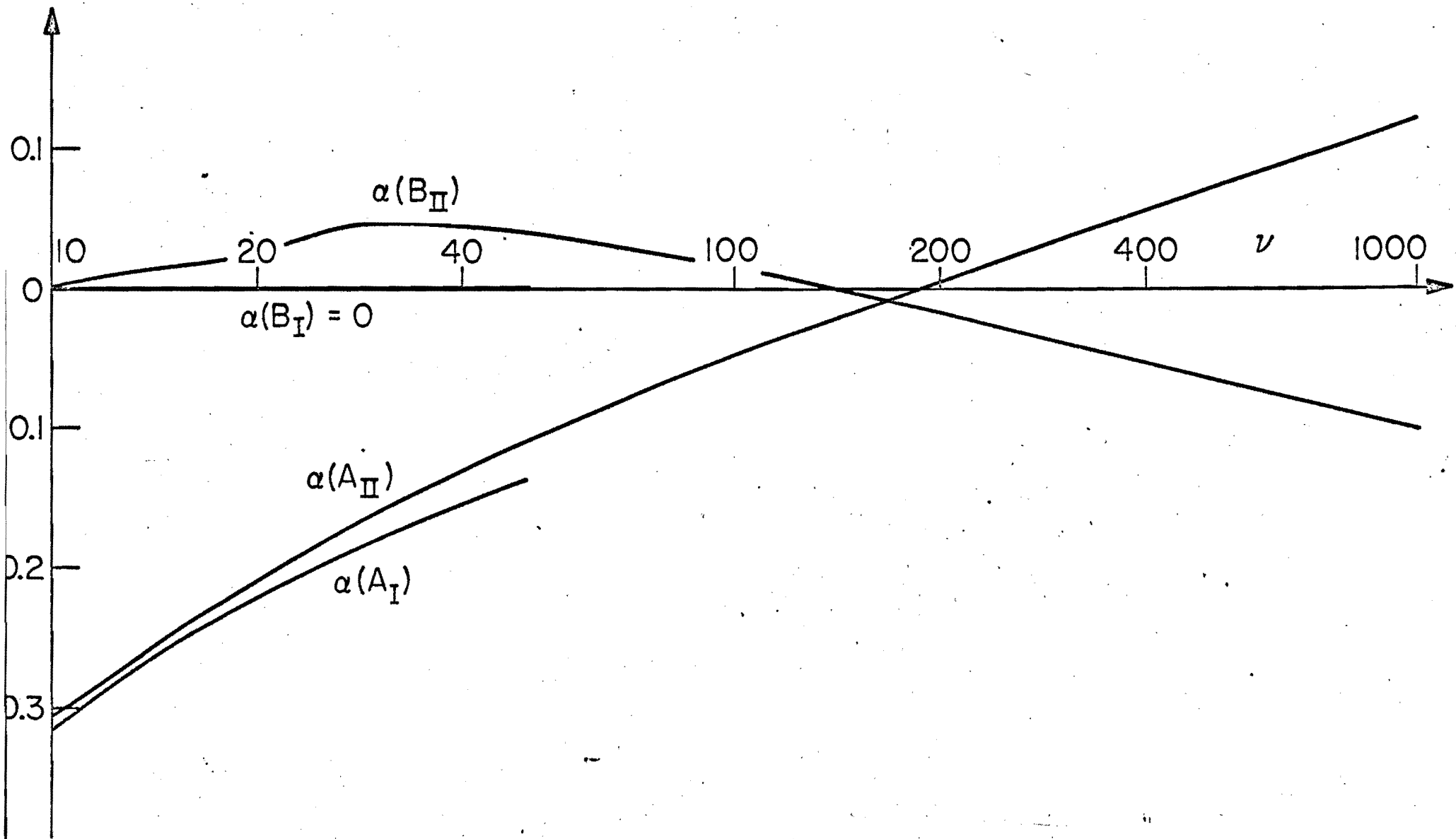


FIG. 1

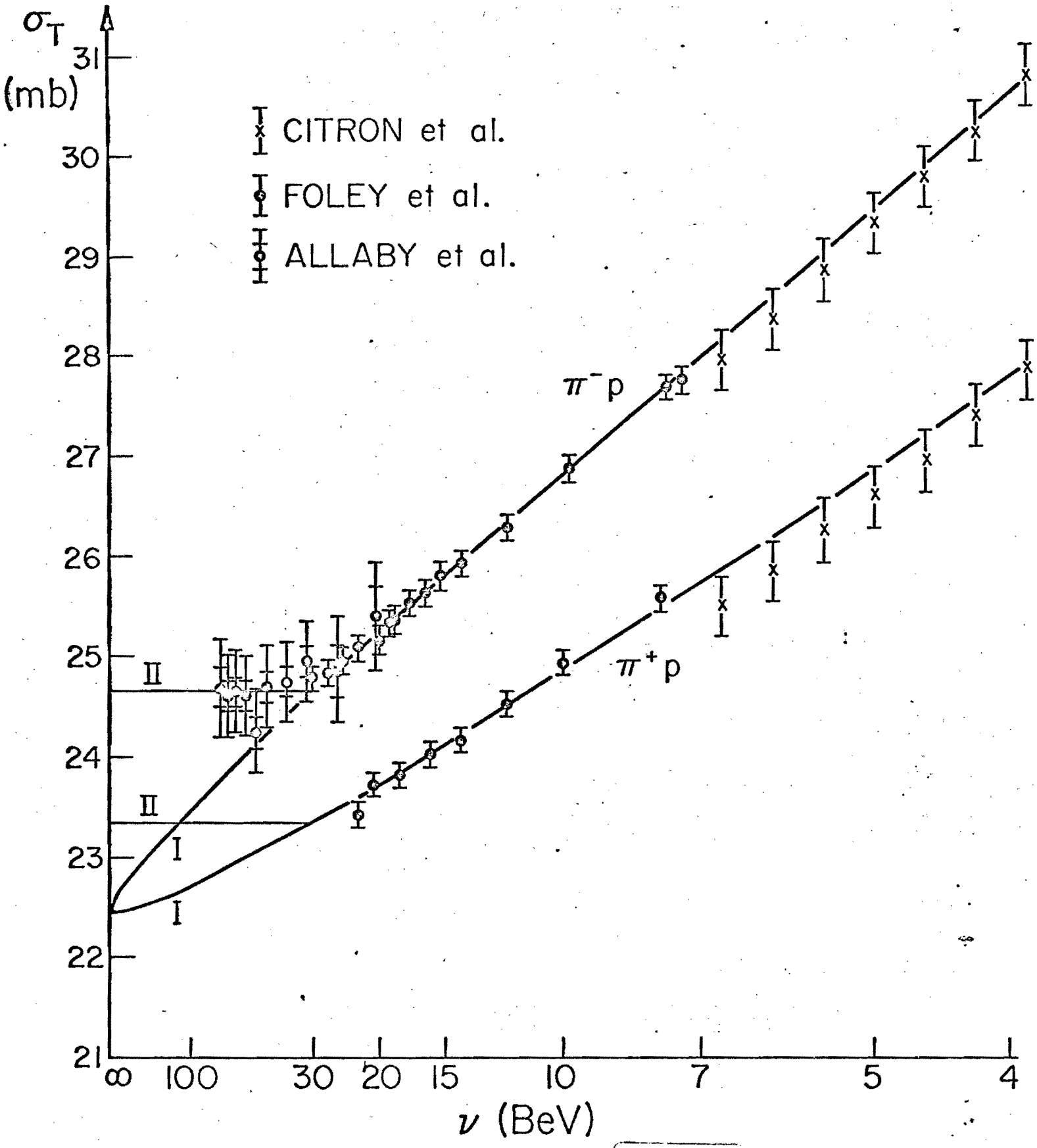
$\sigma_T$
(mb)
31
30
29
28
27
26
25
24
23
22
21
CITRON et al.
FOLEY et al.
ALLABY et al.
$\pi^- p$
$\pi^+ p$
II
II
I
I
∞
100
30
20
15
10
7
5
4
$\nu$ (BeV)

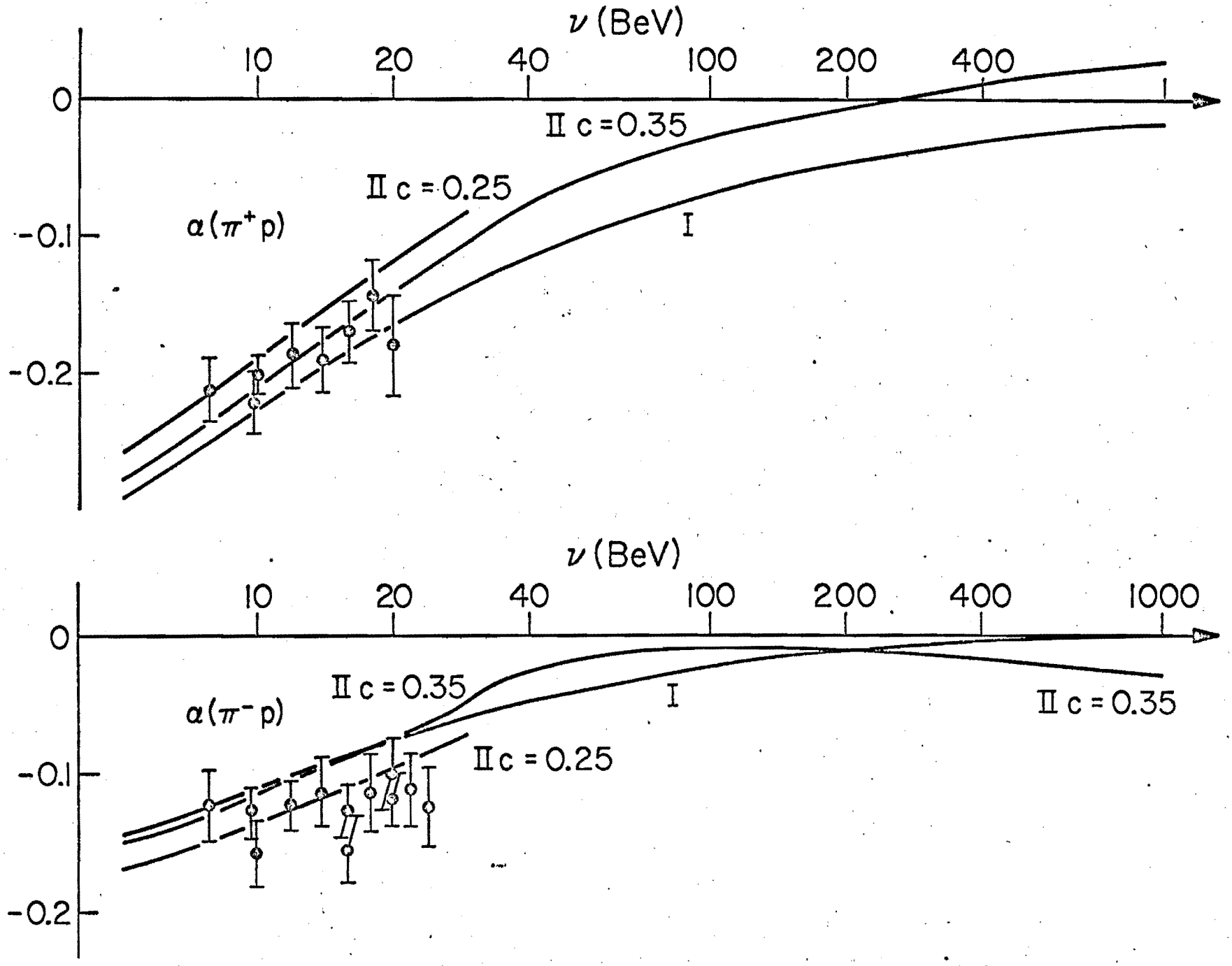
ν (BeV)
10
20
40
100
200
400
0
II c = 0.35
II c = 0.25
α(π⁺p)
I
-0.1
-0.2
ν (BeV)
10
20
40
100
200
400
1000
0
II c = 0.35
α(π⁻p)
I
II c = 0.35
II c = 0.25
-0.1
-0.2

FIG. 3

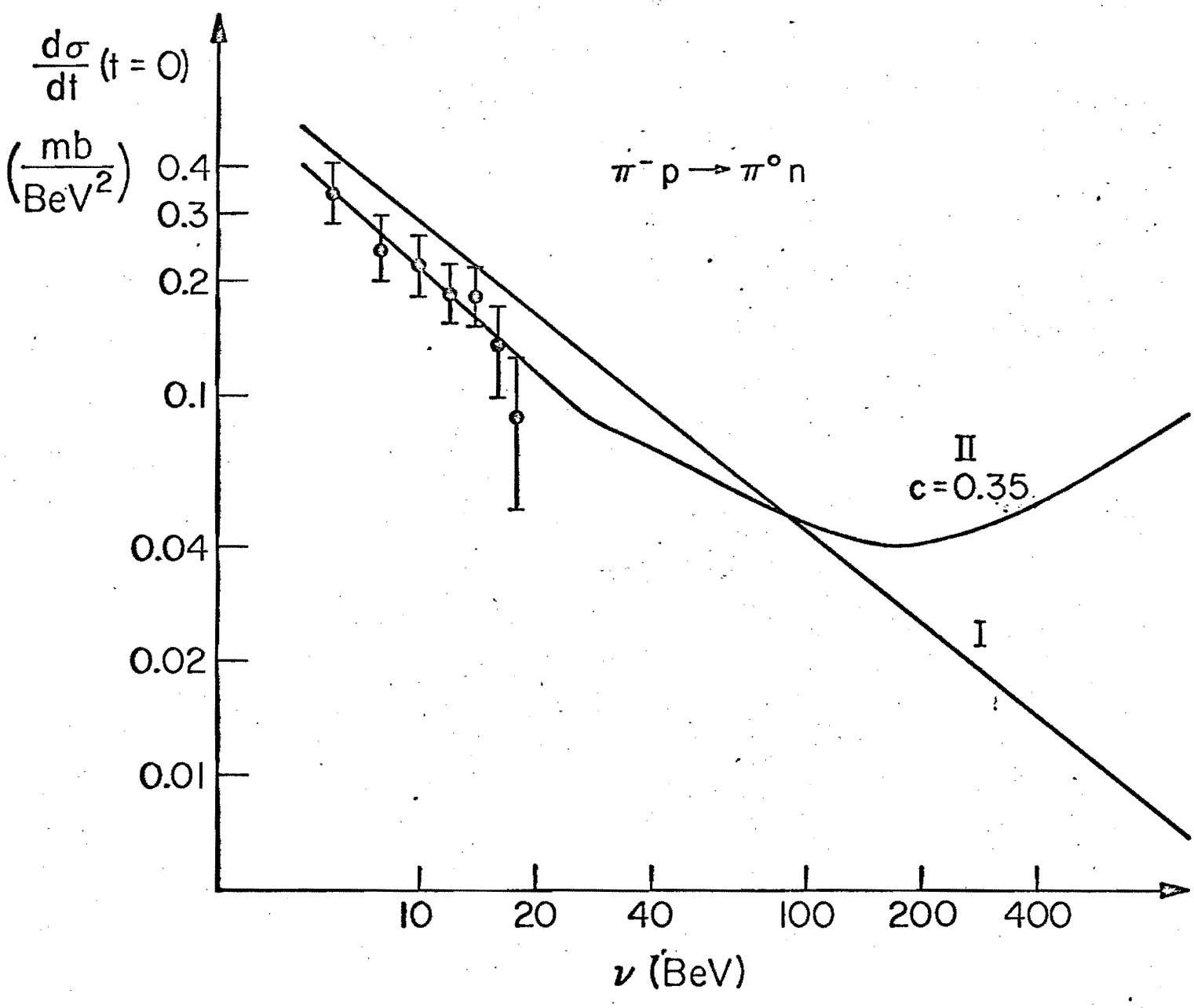
$\frac{d\sigma}{dt}(t=0)$
$\left(\frac{mb}{BeV^2}\right)$
0.4
0.3
0.2
0.1
0.04
0.02
0.01
$\pi^- p \rightarrow \pi^\circ n$
II
c = 0.35
I
10
20
40
100
200
400
$\nu$ (BeV)

FIG. 4

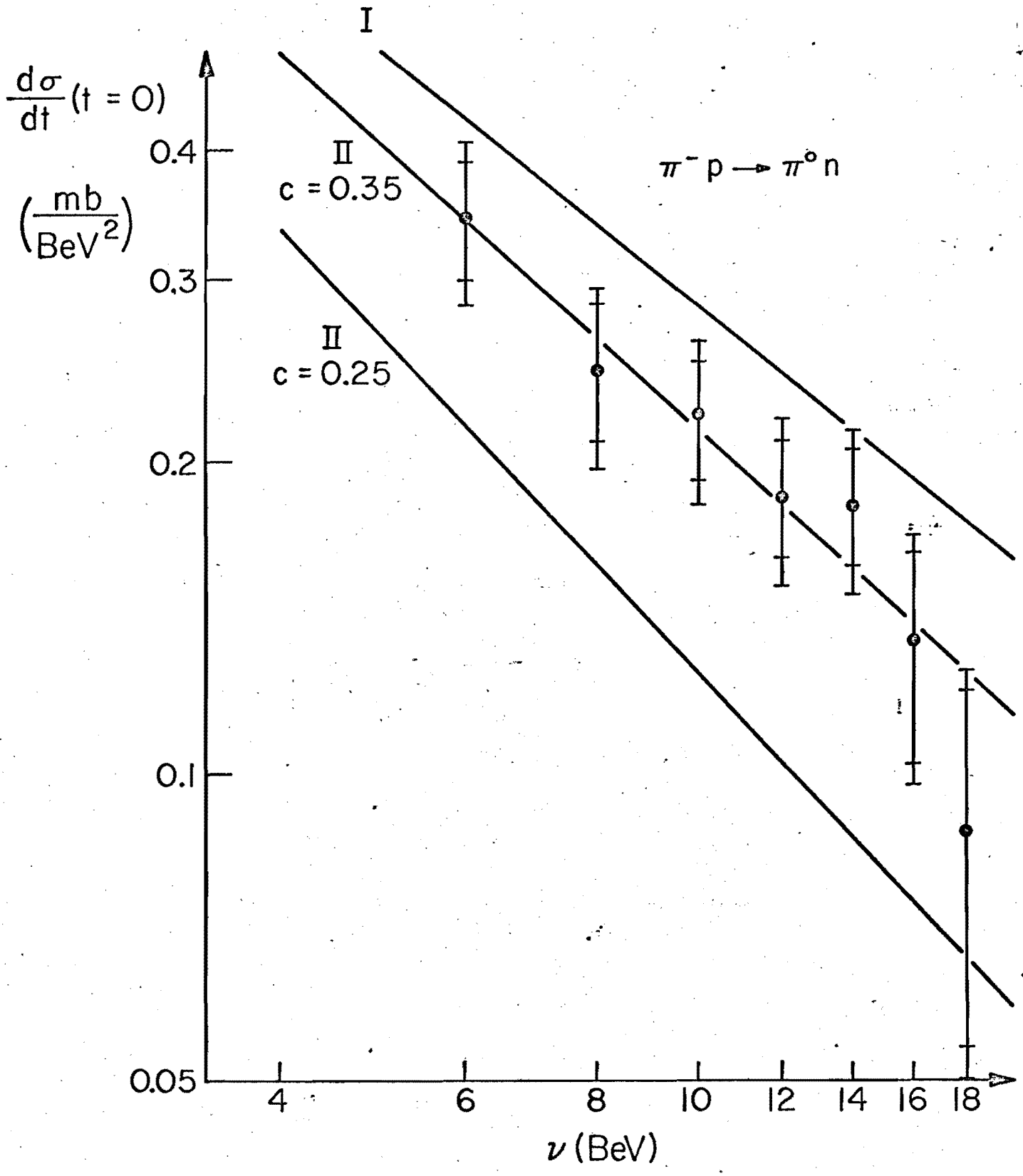
I
II
c = 0.35
II
c = 0.25
$\pi^- p \rightarrow \pi^0 n$
$\frac{d\sigma}{dt}(t=0)$
$\left(\frac{mb}{BeV^2}\right)$
0.4
0.3
0.2
0.1
0.05
4
6
8
10
12
14
16
18
$\nu$ (BeV)

FIG. 5

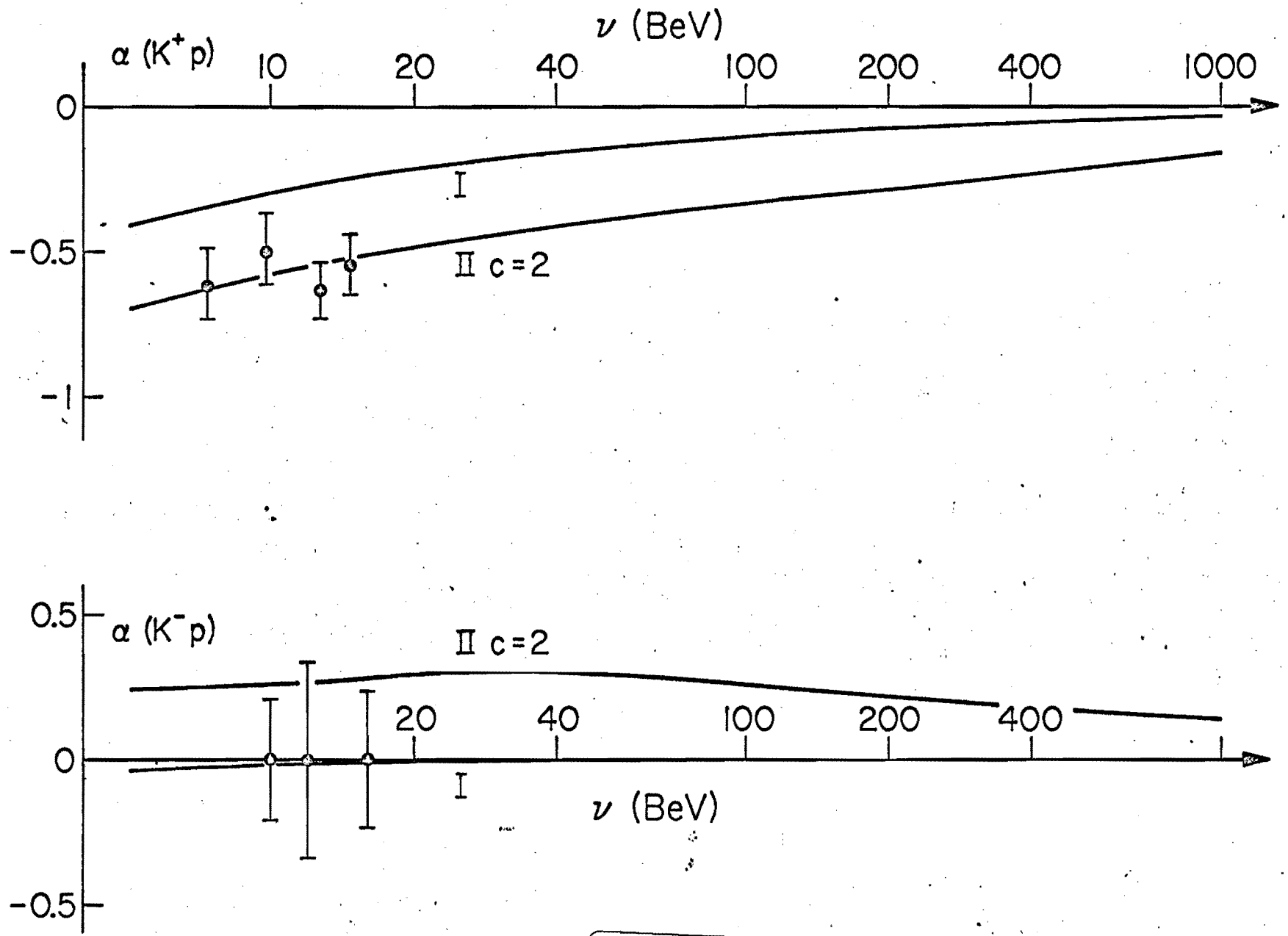
α (K⁺p)
ν (BeV)
10
20
40
100
200
400
1000
0
-0.5
-1
I
II c=2
0.5
α (K⁻p)
II c=2
20
40
100
200
400
0
I
ν (BeV)
-0.5

FIG. 6